Optical orientation of bright excitons in InAs/GaAs quantum dots: Influence of a Faraday magnetic field and the dark exciton states

S. Sancho,[1] M. Chaouache,[1,*] M. A. Maaref,[1] F. Bernardot,[2] B. Eble,[2] A. Lemaître,[3] and C. Testelin[2]

[1]*Unité de Recherche de Physique des Semiconducteurs et Capteurs, Institut Préparatoire aux Etudes Scientifiques et Techniques, BP 51, 2070 La Marsa, Université de Carthage, Tunis, Tunisia*

[2]*Institut des NanoSciences de Paris, UPMC Univ Paris 06, CNRS UMR 7588, 4 Place Jussieu, 75252 Paris cedex 05, France*

[3]*Laboratoire de Photonique et Nanostructures, CNRS, Route de Nozay, F-91460 Marcoussis, France*

(Received 25 April 2011; revised manuscript received 28 September 2011; published 31 October 2011)

We study the injection of polarized bright and dark excitons in quantum dots, under nonresonant or resonant excitation, by polarization-resolved photoluminescence experiments on an ensemble of self-assembled InAs/GaAs quantum dots. The importance of the polarized dark exciton creation on the optical emission under magnetic field is discussed. Under circular excitation, we observe the expected increase and saturation of the polarization rate with a magnetic field applied in Faraday geometry. Strikingly, the polarization rate slightly decreases for magnetic fields greater than ∼1.5 T; the feature is more pronounced for higher interband energies and is attributed to a more efficient initial polarization of the dark exciton states. This interpretation is confirmed by the lack of decrease of the polarization rate for quantum dots excited at exact resonance through a 1LO-phonon-assisted transition. Finally, we measure the bright exciton exchange energy as a function of interband emission energy, we measure a decrease from 65 to 30 μeV in the range 1.28–1.35 eV, and we obtain an estimate of the dark exciton splitting.

DOI: 10.1103/PhysRevB.84.155458 PACS number(s): 75.75.−c, 85.75.−d, 78.20.Ls, 78.66.Fd

I. INTRODUCTION

The studies of spin dynamics in semiconductor quantum dots (QDs) have attracted great interest from both fundamental and practical points of view. In QDs, the spin can be carried by single particles (electron or hole) or by exciton. During the last decade, long spin relaxation times have been observed for excitons,[1] electrons,[2] or holes,[3] supporting proposals for future applications of QDs in spin-dependent devices.

At the same time, optical pumping of nuclear spins in QDs, occurring as a result of the electron–nuclei hyperfine interaction, has been demonstrated[4,5]; an efficient nuclear spin pumping has then been reported and performed in doped QDs.[6] Nonetheless, Maletinsky *et al.*[7] have shown that the nuclear spin relaxation can be greatly enhanced by resident carriers through hyperfine interaction. To overcome this limitation, we need to use neutral QDs. In neutral QDs, the dynamical nuclear polarization (DNP) may strongly depend on the dark exciton population, as recently shown.[8] The control of the polarized dark exciton injection is then important to monitor the DNP in QDs. However, in neutral QDs, the structure of the excited states is more complex than in doped QDs due to the existence of four excitonic states, two bright ones and two dark ones. In a QD, the excitonic fine structure is governed by the exchange interaction between the electron and the hole. This fine structure has been the subject of many studies in recent years,[9–12] a detailed understanding of the exciton fine structure in QDs being of great interest for potential applications in single-photon emitters and entangled two-photon sources for quantum cryptography.[13,14] Moreover, despite numerous studies, interest is still devoted to the exciton spin dynamics, theoretically[15,16] and experimentally, either on single QDs[17] or on QD ensembles.[18]

We report here on the incidence of polarized dark excitons on the QD photoluminescence (PL) polarization, and we give evidence supporting the possibility of injecting significantly polarized dark excitons or avoiding any dark exciton population by choosing nonresonant or resonant excitation. The bright and dark exciton exchange splitting can also be estimated. We then study the anisotropic exchange splitting of the bright exciton states as a function of energy of the interband emission in as-grown QDs, using polarization-resolved PL under a magnetic field applied along the growth axis (Faraday geometry). We measure a decrease of the bright exciton exchange splitting from 65 to 30 μeV in the range 1.28–1.35 eV, a trend already observed in pump-probe experiments on similar QDs.[12] Moreover, while being optically inactive, the dark excitons may play an important role in the polarization of the emitted photons, as previously discussed in type 2 superlattices.[19,20] For the highest emission energies, our experimental data are sensitive to the initial excitation of a nonzero spin polarization of dark excitons, and the PL polarization rate then slightly decreases with increasing magnetic fields >1.5 T. We have developed a theoretical model taking into account the dark exciton contribution to the PL polarization.

II. EXPERIMENTAL DETAILS

We have studied an as-grown sample containing 30 layers of InAs/GaAs QDs with a mean density equal to 4×10^{10} cm^{-2}. QD height and diameter are typically 2–3 and 20 nm, respectively. In continuous wave (cw) PL experiments, the sample was placed at the center of two superconducting coils inside a cryostat filled with liquid helium; the measurements were performed at $T = 2$ K. The magnetic field was oriented parallel to growth axis z of the sample. In the same direction, the cw optical excitation was made using the beam of a 895-nm laser diode focused on the sample; the σ^+ or σ^- circular polarization of the laser beam was controlled by a linear polarizer followed by a Babinet-Soleil compensator, tuned to cause a retardation of $\pm 1/4$ of wavelength between

its eigenaxes. The resultant PL is collected by a lens, the σ^+-polarized emission is selected by an achromatic quarter-wave plate followed by a polarizer, and finally the emission dispersed by a monochromator and detected by a LN_2-cooled charge-coupled device camera. The circular polarization rate of the PL is defined by

$$P_c = \frac{I^{\sigma^+} - I^{\sigma^-}}{I^{\sigma^+} + I^{\sigma^-}}, \tag{1}$$

where $I^{\sigma^+}(I^{\sigma^-})$ denotes the σ^+-polarized PL intensity detected with a σ^+- (σ^--) polarized excitation.

III. EXCITON AND PSEUDOSPIN MODEL

The exciton is made up of an electron in the first conduction band and a hole in the uppermost valence band; for simplification, we consider only heavy-hole states (the heavy- and light-hole states are separated by tens of millielectronvolts). The exciton states are then composed of states with angular-momentum projections $S_z = \pm 1/2$ (for the electron) and $J_z = \pm 3/2$ (for the heavy hole). The resulting four exciton states have momentum projections $M_z = \pm 1$ and ± 2, the quantization axis being normal to the QD plane. The states with $|M_z| = 2$ cannot couple to the light field and are therefore optically inactive (dark excitons), while the states with $|M_z| = 1$ are optically active (bright excitons). Exciton states experience the exchange interaction made of two contributions; the short-range part causes a splitting of the exciton multiplet into bright and dark states (with a dark exciton splitting), while the long-range part results in a splitting of the bright exciton in asymmetric dots, besides contributing to the bright–dark splitting.

In self-assembled InAs/GaAs QDs, the bright excitons form a two-level system that can be considered as a pseudospin 1/2. In an ideal (cylindrical) QD, the eigenstates $|\pm 1\rangle$ are coupled to $\sigma^\pm$ circularly polarized photons, but in an actual QD some symmetry reduction generally lifts the exciton degeneracy by the fine-structure splitting between two linearly polarized states $|X\rangle$ and $|Y\rangle$.[9] This fine-structure splitting has been measured by different techniques, such as micro-PL[9,20] or pump-probe[21,22] measurements.

A magnetic field applied along growth axis z of the sample was used to investigate the behavior versus the field of the excitonic fine-structure splitting. The bright and dark states can be separated into two two-level systems, each of which can be simply described with the use of a pseudospin model.[23]

If we neglect the initial formation of dark excitons and the relaxation between bright and dark excitons, the Hamiltonian describing the bright states can be written as the sum of the exchange and Zeeman terms:

$$H = \frac{\hbar\omega_1}{2}\sigma_x + \frac{\hbar\Omega}{2}\sigma_z, \tag{2}$$

where $\hbar\omega_1$ is the anisotropic exchange splitting of the radiative doublet. We have included a magnetic field B along with the z axis (Faraday geometry) with Larmor frequency; thus, $\Omega = g_X\mu_B B/\hbar$, $g_X = g_h - g_e$ is the exciton longitudinal Landé factor, with g_e and g_h the electron and hole Landé factors, respectively, and σ_i ($i = x, y, z$) are the Pauli matrices.

Within the framework of this model, for a very large exchange interaction compared to the reverse of the spin-relaxation time, we get a simple relation between the PL polarization rate and the applied magnetic field B:

$$P_c(B) = P_c^0 \frac{B^2}{B^2 + (B_1)^2}, \tag{3}$$

where we have defined the effective magnetic field $B_1 = \hbar\omega_1/(g_h - g_e)\mu_B$.

A more complex magnetic field dependence of the PL polarization rate is obtained by considering, in addition, the spin relaxation between the bright $|\pm 1\rangle$ and dark $|\pm 2\rangle$ states, as discussed in Ref. 19. Following Ref. 19, and including the bright/dark exciton relaxation in a four-state basis, we have derived the field dependence of the optical orientation, as presented in Appendix. In the limit of long carrier-spin relaxation times as compared to the bright exciton radiative time, the circular polarization rate $P_c(B)$ takes the following new form:

$$P_c(B) = \frac{B^2}{B^2 + (B_1)^2}\left[P_c^0 + \tilde{P}_c^0 \frac{B^2}{B^2 + (B_2)^2}\right], \tag{4}$$

where the effective field B_2 is $B_2 = d^{1/2}\hbar\omega_2/(g_h + g_e)\mu_B$, $g_h + g_e$ is the longitudinal Landé factor of the dark states, and $\hbar\omega_2$ is their exchange energy splitting. d is a constant >1 (see the Appendix). Eq. (4) is employed to analyze the field dependence of the PL polarization. The parameter sets (B_1, P_c^0) and $(B_2, \tilde{P}_c^0)$ can almost be estimated independently from the low-field ($B < 1$ T) and high-field behaviors, respectively.

IV. RESULTS AND DISCUSSION

Typical PL spectra of our sample are shown in Fig. 1 in a zero magnetic field (Fig. 1(a)) and with $B = 3$ T (Fig. 1(b)). In the experiments, performed at $T = 2$ K, the PL is collected under σ^+ polarization selection and the excitation at 895 nm (1.385 eV) is copolarized (σ^+) or cross polarized (σ^-). The excitation power is 1.2 mW, and the laser-diode beam is focused on the sample in a spot $\sim$200 μm in diameter. The PL spectra are characterized by a full width at half maximum of $\sim$50 meV due to fluctuations of size and shape and strains in the QD ensemble under the spot. The sharp peak at 917 nm (1.352 eV) is attributed to the PL of QDs excited through a 1LO-phonon transition; this feature is exploited later in the analysis of our results (on the contrary, we do not pay attention to the QDs excited with a 2LO-phonon transition, because their PL present only a smooth pattern near 941 nm). In a zero magnetic field (Fig. 1(a)), we repeatedly measure a circular polarization rate of $\sim$4% at 946 nm (1.31 eV); it is attributed to little imperfections of adjustments and of optical components in our experimental setup. At high magnetic fields, e.g., at $B = 3$ T (Fig. 1(b)), the PL polarization rate is typically $\sim$30% in the whole energy range of the QDs—except for the 1LO-phonon–excited QDs, for which it is much higher, as discussed later.

Figure 2 shows the measured circular polarization rate $P_c(B)$ (full circles) as function of magnetic field for several detection wavelengths within the emission band of the QDs: $\lambda_{\text{det}} = 930$, 940, 950, and 960 nm. As Eq. (3) predicts, $P_c(B)$ increases with magnetic field B; the continuous lines in Fig. 2

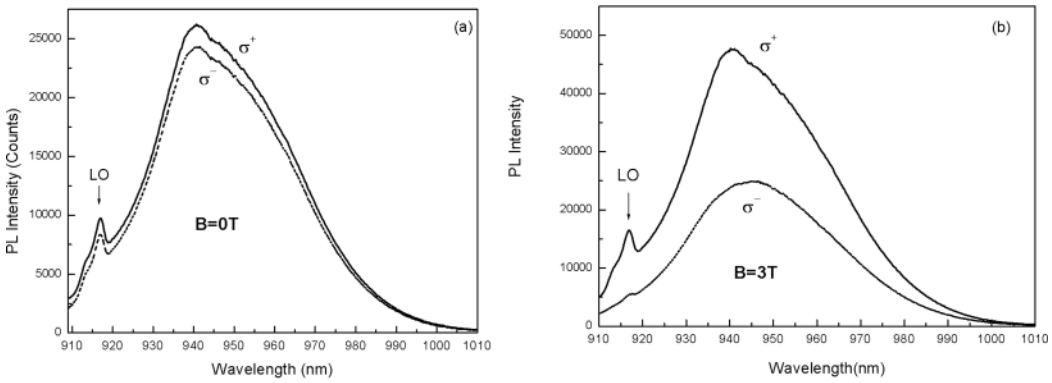

FIG. 1. σ^+ polarization-resolved PL spectra of our InAs QDs under cw excitation at $E_{\text{exc}} = 1.385$ eV ($\lambda_{\text{exc}} = 895$ nm) with σ^+ (solid line) and σ^- (dashed line) polarized light, at $T = 2$ K, (a) in a zero magnetic field and (b) with $B = 3$ T.

are fits of the experimental data with Eq. (3) within a small constant shift due to the nonzero experimental $P_c(B = 0)$. We then deduce a B_1 parameter for each studied wavelength. B_1 versus wavelength is reported in Fig. 3. In the same graph, the bright exciton splitting $\hbar\omega_1$ is specified; assuming a bright exciton Landé factor $g_X = g_h - g_e = 2.3$,[24,26] $\hbar\omega_1$ decreases from 65 to 30 μeV in the range 1.28–1.35 eV of the emission energies of the QDs. Such behavior has been previously observed on similar QDs,[12] revealing the importance of piezoelectricity.[10]

As observed in Fig. 2, the polarization rate $P_c(B)$ decreases at high fields. We then analyzed the PL intensity at $\lambda_{\text{det}} = 917$ nm, 1LO-phonon energy below the excitation. Under σ^+-polarized excitation, two contributions have to be considered[27]: (1) a resonant excitation, with the creation of one LO phonon and an efficient $|+1\rangle$ exciton injection,[25,28] and (2) a nonresonant excitation, with the creation of bright and dark excitons through an energy relaxation of the carriers via acoustic phonons. From the PL spectra, we extracted both contributions, and the circular polarization rates are given in Fig. 4(a) and (b) for nonresonant and resonant excitations, respectively. For the nonresonant contribution (Fig. 4(a)), $P_c(B)$ decreases at high field, as it does for lower-energy PL polarization rates (see Fig. 2). On the contrary, for the resonant excitation and an efficient $|+1\rangle$ bright exciton injection, we clearly see that $P_c(B)$ saturates at high field and remains constant at a high-level rate. These behaviors can be explained by considering the dependence between parameters P_c^0 and $\tilde{P}_c^0$ on the excitation. For the resonant excitation, no dark exciton is photocreated, so $G_{22} = G_{-2-2} = 0$ and $\tilde{P}_c^0 = 0$ (see the Appendix). According to Eq. (4), the, circular polarization rate saturates at P_c^0 (close to 80% in our sample). For the nonresonant excitation, dark excitons are created, particularly because the excited-hole-spin relaxation is fast while $S_z = -1/2$ electrons keep part of their polarization. This leads to $G_{-2-2} > G_{22}$ and $\tilde{P}_c^0 < 0$ (see the Appendix). From Eq. (4), we then expect an increase of the PL polarization rate at low field, followed at higher field by a decrease due to the field dependence of the factor in square brackets; this behavior of the polarization rate is the one observed in Fig. 4(a). Under nonresonant or resonant excitations, different polarized exciton populations, which could induce some DNP,

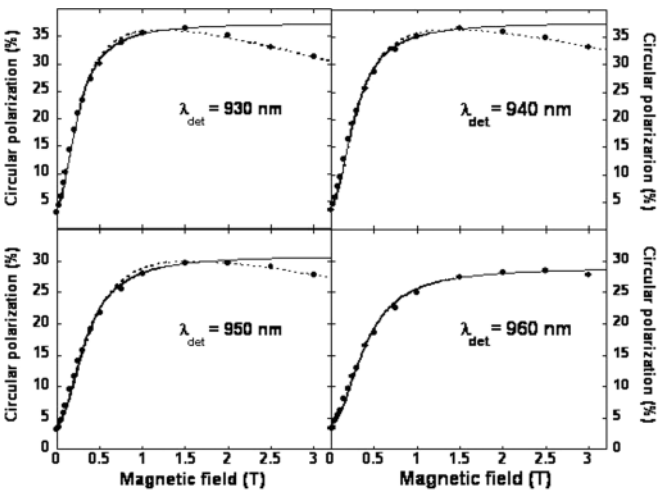

FIG. 2. Longitudinal magnetic field dependence of the PL polarization rate at different emission energies of the QDs. The detection wavelengths are specified. Solid and dashed lines are fits obtained with Eqs. (3) and (4), respectively. The fitting parameters are, respectively, $P_c^0 = 35\%$, 34.8%, 29%, and 24.8% and $B_1 = 0.25$, 0.30, 0.34, and 0.40 T for $\lambda_{\text{det}} = 930$, 940, 950, and 960 nm; also, $\tilde{P}_c^0 = -30\%$, -25%, and -22% and $B_2 = 5$, 5.3, and 5.6 T for $\lambda_{\text{det}} = 930$, 940, and 950 nm.

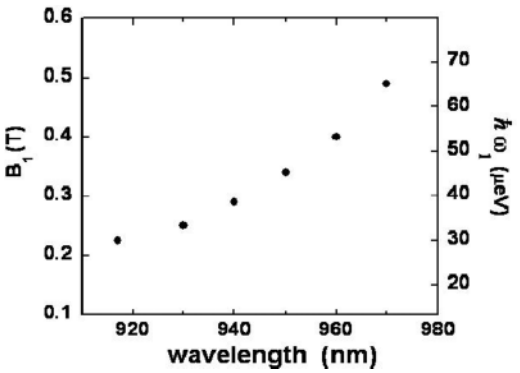

FIG. 3. Effective magnetic field B_1 and bright exciton exchange splitting $\hbar\omega_1$ (assuming $g_X = g_h - g_e = 2.3$). We can observe a monotonic decrease from $\hbar\omega_1 = 65$ μeV at 1.28 eV to $\hbar\omega_1 = 30$ μeV at 1.35 eV.

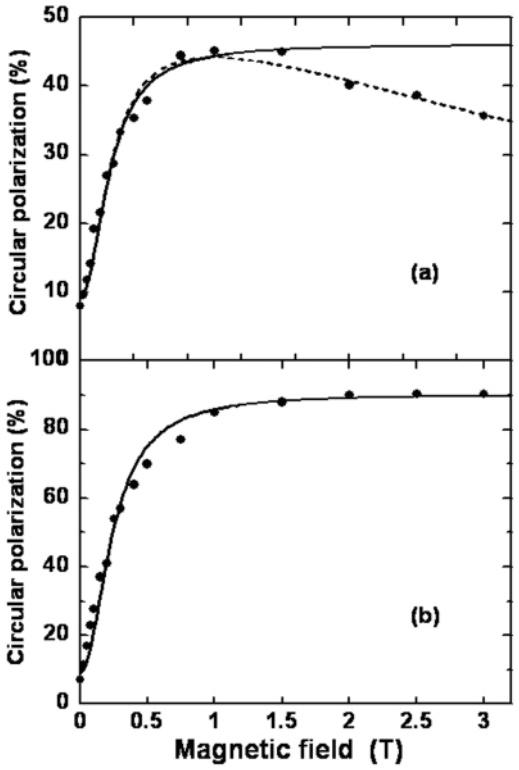

FIG. 4. Longitudinal magnetic field dependence of the PL polarization rate at $\lambda_{det} = 917$ nm, for (a) a nonresonant excitation and (b) a resonant excitation. Solid and dashed lines are fits obtained with Eqs. (3) and (4), respectively. The fitting parameters are (a) $P_c^0 = 39\%$, $B_1 = 0.23$ T and $\tilde{P}_c^0 = -30.5\%$, $B_2 = 3.7$ T and (b) $P_c^0 = 81.3\%$, $B_1 = 0.24$ T.

are created. Despite different exciton populations, which should induce different nuclear fields, similar magnetic field dependence is observed for both excitation configurations. Moreover, the PL polarization is power-density independent on one order of magnitude. We then reasonably assumed that there is no significant DNP.

Another point to consider is a possible influence of an anticrossing between the $|-1\rangle$ and $|-2\rangle$ (or $|+2\rangle$) states, which could alter the PL polarization. Such anticrossing happens for a magnetic field B_c satisfying the condition $\delta_0 = |g_e|\,\mu_B B_c$ ($\delta_0 = g_h \mu_B B_c$), where δ_0 is the bright-dark exciton splitting. From the emission energy dependence of the PL polarization (Fig. 2), we expect a decrease of this critical field when the emission energy increases. This behavior is not in agreement with the increase of δ_0 observed when the QD size decreases (and the emission energy increases).[9] Moreover, in Ref. 9, no decrease of the PL polarization was observed after saturation, despite evidence of anticrossing. In the framework of our model (see the Appendix), such behavior could be explained by a nonradiative γ_0 rate larger than the electron (hole) relaxation rate γ_e (γ_h) (leading to parameter $c \approx 0$, in Eq. (A6)). Finally, a possible effect of a differential thermal occupation of the $|+1\rangle$ and $|-1\rangle$ states, which should favor the $|-1\rangle$ state in an increasing field, has to be excluded because no such decrease appears at 917 nm for a resonant excitation (whereas it does for a nonresonant excitation at the same energy; see Fig. 4).

In Figs. 2 and 4(a), the measured polarization rate has been fitted with Eq. (4) (dashed lines)—still within a constant shift. The previous B_1 parameters are negligibly perturbed. From the fitting curves shown in Figs. 2 and 4(a), we can estimate that B_2 varies from 5.6 T at 950 nm to 3.7 T at 917 nm with a 20% uncertainty. We can deduce that the dark exciton exchange splitting decreases when the QD emission energy increases, as it does for the bright exciton. Using the values $g_h = 1.5$ and $g_e = -0.8$, previously measured on similar QDs,[24] we obtained a typical dark exciton exchange splitting of $\hbar\omega_2 \approx \frac{160\pm30}{\sqrt{d}}$ μeV. Taking into account the uncertainty on the Landé factors and the B_2 parameters, and a possible value $d > 1$, this dark exciton exchange splitting is on the order of previous measurements: $\hbar\omega_2 = 0$–90 μeV on InAs/GaAs QDs.[9]

V. CONCLUSION

We have studied the influence of a spin-polarization of dark excitons on the PL circular polarization of self-assembled InAs/GaAs QDs. By comparing the Faraday magnetic field dependence of the PL polarization rate, without a photocreated dark exciton or with a spin-polarized dark exciton population (under resonant or nonresonant optical excitation, respectively), we have clearly observed different behaviors of the PL polarization rate, which are quantitatively explained in the framework of a model including relaxation processes between the bright and the dark excitons. The fine structure of the bright and dark excitons has also been estimated from the analysis of polarized PL, under Faraday magnetic field, for nonresonant and resonant circularly polarized excitation. In the QD emission range, a decrease of the bright exciton exchange splitting is observed when the QD emission energy increases.

ACKNOWLEDGMENTS

This work is supported by the French–Tunisian Project No. 09-G-1307, funded by the Comité Mixte pour la Coopération Universitaire.

APPENDIX

The optical orientation of excitons can be described by using the density-matrix formalism. We use the procedure drawn in Ref. 19. In the steady-state regime under photoexcitation, the density matrix satisfies the kinetic equation

$$\left(\frac{\partial\rho}{\partial t}\right)_{\text{rec}} + \left(\frac{\partial\rho}{\partial t}\right)_{\text{rel}} + \frac{i}{\hbar}\left[\rho, H_{\text{exch}} + H_Z\right] + \hat{G} = 0. \quad \text{(A1)}$$

The left-hand terms take account of the exciton recombination, the spin relaxation, the exchange, and the Zeeman interaction; $\hat{G}$ is the generation matrix associated with the photoexcitation. On the basis of $M_z = +2, +1, -1$, or -2, the exchange Hamiltonian is given by

$$H_{\text{exch}} = \frac{\hbar}{2}\begin{pmatrix} -2\omega_0 & 0 & 0 & \omega_2 \\ 0 & 0 & \omega_1 & 0 \\ 0 & \omega_1 & 0 & 0 \\ \omega_2 & 0 & 0 & -2\omega_0 \end{pmatrix}. \quad \text{(A2)}$$

For a longitudinal magnetic field, the Zeeman Hamiltonian is written as

$$H_Z = \frac{1}{2}\mu_B B_z \begin{pmatrix} (g_h+g_e) & 0 & 0 & 0 \\ 0 & (g_h-g_e) & 0 & 0 \\ 0 & 0 & -(g_h-g_e) & 0 \\ 0 & 0 & 0 & -(g_h+g_e) \end{pmatrix}, \tag{A3}$$

with g_h and g_e as the hole and electron Landé factors, respectively.

We assume $G_{mm'} = 0$ for the pairs $m = \pm 1$, $m' = \pm 2$ or $m = \pm 2$, $m' = \pm 1$—or $m = -m' = \pm 2$. Under resonant excitation, the excitons are created directly into the states $M_z = \pm 1$ so that $G_{mm'} \neq 0$ only for $m, m' = \pm 1$. Under nonresonant excitation, an exciton can be formed after spin relaxation of the photocreated exciton or by binding of an electron and a hole, which may not be created by the same photon; in this case, all diagonal components of $\hat{G}$ may be nonzero. For resonant or nonresonant circular excitation, no coherence is generated between states $M_z = +1$ and -1, so $G_{\pm 1 \mp 1} = 0$. We can define (1) the radiative rate γ_r of bright excitons and the nonradiative rate γ_0 of excitons, (2) the spin relaxation rate γ_X between bright excitons $+1$ and -1, (3) the spin relaxation rates γ_e between the ± 1 and ± 2 states and γ_h between the ± 1 and ∓ 2 states, and (4) the decoherence rates $\gamma_X^{(2)}$ and $\gamma_D^{(2)}$ of the nondiagonal density-matrix components ρ_{+1-1} and ρ_{+2-2}, respectively. The γ_r and γ_0 rates define the first term in Eq. (A1); the other rates define the second term of this equation.

From the solution of Eq. (A1), it is possible to determine the field dependence of the PL polarization rate. Under circular excitation, the circular polarization rate can be written as

$$P_c = N\frac{\Gamma_r}{\Gamma_X}\frac{\left[1+\left(\frac{\Omega_{//}}{\tilde{\Gamma}_X}\right)^2\right]\left[P_c^0 + Q\tilde{P}_c^0\right]}{\left[1+\left(\frac{\Omega_{//}}{\tilde{\Gamma}_X}\right)^2\right][1-S] + \frac{(\omega_1)^2}{\Gamma_X\tilde{\Gamma}_X}}, \tag{A4}$$

with

$$Q = \frac{\Gamma_-}{\Gamma_0}\frac{1+\left(\frac{\Omega'_{//}}{\tilde{\Gamma}_D}\right)^2}{1+\left(\frac{\Omega'_{//}}{\tilde{\Gamma}_D}\right)^2 + \frac{(\omega_2)^2}{\Gamma_0\tilde{\Gamma}_D}}, \quad S = \frac{\Gamma_-}{\Gamma_X}Q,$$

$$N = \frac{1-\frac{\Gamma_+^2}{\Gamma_0\Gamma_r}}{1+\frac{\Gamma_+}{\Gamma_0}p}, \quad P_c^0 = \frac{G_{+1+1}-G_{-1-1}}{G_{+1+1}+G_{-1-1}},$$

$$\tilde{P}_c^0 = \frac{G_{+2+2}-G_{-2-2}}{G_{+1+1}+G_{-1-1}} \quad \text{and} \quad p = \frac{G_{+2+2}+G_{-2-2}}{G_{+1+1}+G_{-1-1}}. \tag{A5}$$

The Larmor frequencies $\Omega_{//}$ and $\Omega'_{//}$ are related to the Zeeman splitting of the bright and dark excitons, respectively: $\hbar\Omega_{//} = (g_h - g_e)\mu_B B_z$ and $\hbar\Omega'_{//} = (g_h + g_e)\mu_B B_z$. The Γ rates are defined by $\Gamma_\pm = \gamma_e \pm \gamma_h$, $\Gamma_0 = \gamma_0 + \Gamma_+$, $\Gamma_r = \gamma_r + \Gamma_0$, $\Gamma_X = 2\gamma_X + \Gamma_r$, $\tilde{\Gamma}_D = \Gamma_0 + \gamma_D^{(2)}$, and $\tilde{\Gamma}_X = \Gamma_r + \gamma_X^{(2)}$.

Assuming a radiative rate γ_r large compared to the relaxation rates γ_e and γ_h,[1] we have $S << 1$. Moreover, we can assume that the exchange and Zeeman splittings are large compared to the rate terms. We can finally write

$$P_c = a\frac{(\Omega_{//})^2}{(\Omega_{//})^2 + b(\omega_1)^2}\left[P_c^0 + Q\tilde{P}_c^0\right],$$

with

$$Q = c\frac{(\Omega'_{//})^2}{(\Omega'_{//})^2 + d\,(\omega_2)^2},$$

$$a = \frac{\Gamma_r}{\Gamma_X} = \frac{\gamma_r+\gamma_0+\gamma_e+\gamma_h}{2\gamma_X+\gamma_r+\gamma_0+\gamma_e+\gamma_h},$$

$$b = \frac{\tilde{\Gamma}_X}{\Gamma_X} = \frac{\gamma_X^{(2)}+\gamma_r+\gamma_0+\gamma_e+\gamma_h}{2\gamma_X+\gamma_r+\gamma_0+\gamma_e+\gamma_h},$$

$$c = \frac{\Gamma_-}{\Gamma_0} = \frac{\gamma_e-\gamma_h}{\gamma_0+\gamma_e+\gamma_h},$$

and

$$d = \frac{\tilde{\Gamma}_D}{\Gamma_0} = \frac{\gamma_D^{(2)}+\gamma_0+\gamma_e+\gamma_h}{\gamma_0+\gamma_e+\gamma_h}. \tag{A6}$$

These constants verify the following conditions: $a, c \leqslant 1$ and $d \geqslant 1$. Particular conditions can be noticed: (1) the relation $a \approx b \approx 1$ is verified when the radiative rate γ_r is larger than the other rates[15]; (2) for the typical QD size, the γ_e rate is larger than the γ_h one[16] ($\gamma_e >> \gamma_h$), so for a negligible nonradiative rate γ_0, $c \approx 1$; and (3) the bright exciton spin relaxation rate γ_X is small compared to the radiative rate γ_r[1] at low temperature, $a = 1$. We have then assumed $a = b = c = 1$ and $d \geqslant 1$ in the derivation of Eqs. (3) and (4).

*moncef_chaouache@yahoo.fr

[1] M. Paillard, X. Marie, P. Renucci, T. Amand, A. Jbeli, and J.-M. Gérard, Phys. Rev. Lett. **86**, 1634 (2001).

[2] M. Kroutvar, Y. Ducommun, D. Heiss, M. Bichler, D. Schuh, G. Abstreiter, and J. J. Finley, Nature **432**, 81 (2004).

[3] D. Heiss, S. Schaeck, H. Huebl, M. Bichler, G. Abstreiter, J. J. Finley, D. V. Bulaev, and D. Loss, Phys. Rev. B **76**, 241306(R) (2007).

[4] D. Gammon, A. L. Efros, T. A. Kennedy, M. Rosen, D. S. Katzer, D. Park, S. W. Brown, V. L. Korenev, and I. A. Merkulov, Phys. Rev. Lett. **86**, 5176 (2001).

[5]B. Eble, O. Krebs, A. Lemaître, K. Kowalik, K. Kudelski, P. Voisin, B. Urbaszek, X. Marie, and T. Amand, Phys. Rev. B **74**, 081306 (2006).
[6]B. Urbaszek, P.-F. Braun, T. Amand, O. Krebs, T. Belhadj, A. Lemaítre, P. Voisin, and X. Marie, Phys. Rev. B **76**, 201301 (2007).
[7]P. Maletinsky, A. Badolato, and A. Imamoglu, Phys. Rev. Lett. **99**, 056804 (2007).
[8]E. A. Chekhovich, A. B. Krysa, M. S. Skolnick, and A. I. Tartakovskii, Phys. Rev. B **83**, 125318 (2011).
[9]M. Bayer, G. Ortner, O. Stern, A. Kuther, A. A. Gorbunov, A. Forchel, P. Hawrylak, S. Fafard, K. Hinzer, T. L. Reinecke, S. N. Walck, J. P. Reithmaier, F. Klopf, and F. Schäfer, Phys. Rev. B **65**, 195315 (2002) and reference therein.
[10]R. Seguin, A. Schliwa, S. Rodt, K. Pötschke, U. W. Pohl, and D. Bimberg, Phys. Rev. Lett. **95**, 257402 (2005).
[11]G. Bester, X. Wu, D. Vanderbilt, and A. Zunger, Phys. Rev. Lett. **96**, 187602 (2006).
[12]C. Testelin, E. Aubry, M. Chaouache, M. Maaref, F. Bernardot, M. Chamarro, J.-M. Gérard, and R. Ferreira, Phys. Status Solidi **3**, 3900 (2006); **4**, 1385 (2007).
[13]D. Loss and D. P. DiVincenzo, Phys. Rev. A **57**, 120 (1998).
[14]O. Benson, C. Santori, M. Pelton, and Y. Yamamoto, Phys. Rev. Lett. **84**, 2513 (2000).
[15]K. Roszak, V. M. Axt, T. Kuhn, and P. Machnikowski, Phys. Rev. B **76**, 195324 (2007).
[16]Y. H. Liao, J. I. Climente, and S. J. Cheng, Phys. Rev. B **83**, 165317 (2011).
[17]R. Kaji, S. Adachi, T. Shindo, and S. Muto, Phys. Rev. B **80**, 235334 (2009).
[18]J. Johansen, B. Julsgaard, S. Stobbe, J. M. Hvam, and P. Lodahl, Phys. Rev. B **81**, 081304(R) (2010).
[19]R. I. Dzhioev, H. M. Gibbs, E. L. Ivchenko, G. Khitrova, V. L. Korenev, M. N. Tkachuk, and B. P. Zakharchenya, Phys. Rev. B **56**, 13405 (1997).
[20]J. J. Finley, D. J. Mowbray, M. S. Skolnick, A. D. Ashmore, C. Baker, A. F. G. Monte, and M. Hopkinson, Phys. Rev. B **66**, 153316 (2002).
[21]F. Bernardot, E. Aubry, J. Tribollet, C. Testelin, M. Chamarro, L. Lombez, P.-F. Brauun, X. Marie, T. Amand, and J.-M. Gérard, Phys. Rev. B **73**, 085301 (2006).
[22]I. A. Yugova, A. Greilich, E. A. Zhukov, D. R. Yakovlev, M. Bayer, D. Reuter, and A. D. Wieck, Phys. Rev. B **75**, 195325 (2007).
[23]R. I. Dzhioev, B. P. Zakharchenya, E. L. Ivchenko, V. L. Korenev, Yu. G. Kusraev, N. N. Ledentsov, V. M. Ustinov, A. E. Zhukov, and A. F. Tsatsul'nikov, Phys. Sol. State **40**, 790 (1998).
[24]P. Desfonds, B. Eble, F. Fras, C. Testelin, F. Bernardot, M. Chamarro, B. Urbaszek, T. Amand, X. Marie, J.-M. Gérard, V. Thierry-Mieg, A. Miard, and A. Lemaître, Appl. Phys. Lett. **96**, 172108 (2010).
[25]M. Sénès, B. Urbaszek, X. Marie, T. Amand, J. Tribollet, F. Bernardot, C. Testelin, M. Chamarro, and J.-M. Gérard, Phys. Rev. B **71**, 115334 (2005).
[26]We have measured this typical bright exciton Landé factor on similarly grown QDs, not mentioned in Refs. 16 and 24, in the emission energy range 915–930 nm, either by time-resolved PL or by dichroïsm technique under magnetic field.
[27]M. J. Steer, D. J. Mowbray, W. R. Tribe, M. S. Skolnick, M. D. Sturge, M. Hopkinson, A. G. Cullis, C. R. Whitehouse, and R. Murray, Phys. Rev. B **54**, 17738 (1996).
[28]I. V. Ignatiev, I. E. Kozin, V. G. Davydov, S. V. Nair, J. S. Lee, H. W. Ren, S. Sugou, and Y. Masumoto, Phys. Rev. B **63**, 075316 (2001); I. V. Ignatiev, I. E. Kozin, S. V. Nair, H. W. Ren, S. Sugou, and Y. Masumoto, *ibid.* **61**, 15633 (2000).